

## RESEARCH ARTICLE

# Gene regulation analysis of patient-derived iPSCs and its CRISPR-corrected control provides a new tool for studying perturbations of *ELMOD3* c.512A>G mutation during the development of inherited hearing loss

Xianlin Liu<sup>1,2</sup>, Jie Wen<sup>3,4</sup>, Xuezhong Liu<sup>5</sup>, Anhai Chen<sup>1,2</sup>, Sijun Li<sup>1,2</sup>, Jing Liu<sup>1,2</sup>, Jie Sun<sup>6</sup>, Wei Gong<sup>3,4</sup>, Xiaoming Kang<sup>3,4</sup>, Zhili Feng<sup>3,4</sup>, Chufeng He<sup>1,2</sup>, Lingyun Mei<sup>1,2</sup>, Jie Ling<sup>7\*</sup>, Yong Feng<sup>1,3,4\*</sup>

**1** Department of Otolaryngology, Xiangya Hospital, Central South University, Changsha, Hunan, China, **2** Key Laboratory of Otolaryngology Major Disease Research of Hunan Province, Changsha, Hunan, China, **3** Department of Otolaryngology Head and Neck Surgery, The Affiliated Changsha Central Hospital, Hengyang Medical School, University of South China, Changsha, Hunan, China, **4** Institute of Otolaryngology Head and Neck Surgery, University of South China, Changsha, Hunan, China, **5** Department of Otolaryngology, University of Miami Miller School of Medicine, Miami, FL, United States of America, **6** Department of Otolaryngology Head and Neck Surgery, The Eighth Affiliated Hospital, Sun Yat-sen University, Futian District, Shenzhen, China, **7** Medical Functional Experiment Center, School of Basic Medical Science, Central South University, Changsha, Hunan, China

\* [lingjie@sklmg.edu.cn](mailto:lingjie@sklmg.edu.cn) (JL); [fengyong\\_hn@hotmail.com](mailto:fengyong_hn@hotmail.com) (YF)



## OPEN ACCESS

**Citation:** Liu X, Wen J, Liu X, Chen A, Li S, Liu J, et al. (2023) Gene regulation analysis of patient-derived iPSCs and its CRISPR-corrected control provides a new tool for studying perturbations of *ELMOD3* c.512A>G mutation during the development of inherited hearing loss. PLoS ONE 18(9): e0288640. <https://doi.org/10.1371/journal.pone.0288640>

**Editor:** Michal Hetman, University of Louisville, UNITED STATES

**Received:** November 14, 2022

**Accepted:** June 30, 2023

**Published:** September 14, 2023

**Copyright:** © 2023 Liu et al. This is an open access article distributed under the terms of the [Creative Commons Attribution License](https://creativecommons.org/licenses/by/4.0/), which permits unrestricted use, distribution, and reproduction in any medium, provided the original author and source are credited.

**Data Availability Statement:** All relevant data are within the manuscript and its [Supporting Information](#) files.

**Funding:** This work was supported by the National Key Research and Development Program of China [Grant No. 2020YFC2005204] awarded to YF; the National Natural Science Foundation of China [Grant No. 82101233, 82271187 and 82071065]; the Startup Project from the University of South

## Abstract

The *ELMOD3* gene is implicated in causing autosomal recessive/dominant non-syndromic hearing loss in humans. However, the etiology has yet to be completely elucidated. In this study, we generated a patient-derived iPSC line carrying *ELMOD3* c.512A>G mutation. In addition, the patient-derived iPSC line was corrected by CRISPR/Cas9 genome editing system. Then we applied RNA sequencing profiling to compare the patient-derived iPSC line with different controls, respectively (the healthy sibling-derived iPSCs and the CRISPR/Cas9 corrected iPSCs). Functional enrichment and PPI network analysis revealed that differentially expressed genes (DEGs) were enriched in the gene ontology, such as sensory epithelial development, intermediate filament cytoskeleton organization, and the regulation of ion transmembrane transport. Our current work provided a new tool for studying how disruption of *ELMOD3* mechanistically drives hearing loss.

## Introduction

Human perception of sound depends on the refined structure of the cochlea, and the auditory sensory epithelium is the specialized region of the cochlea that transduces sound [1]. The organ of Corti located in the cochlea, contains one row of inner hair cells (IHCs) and three

China [Grant No. 201RGC002]; the University of South China Clinical Research 4310 Program; the Fundamental Research Funds for the Central Universities of Central South University [Grant No. 1053320190364]; the Natural Science Foundation of Hunan Province [Grant No. 2022JJ30506]. The funders had no role in study design, data collection and analysis, decision to publish, or preparation of the manuscript.

**Competing interests:** The authors have declared that no competing interests exist.

rows of outer hair cells (OHCs) [2]. The hair cells are lined with rows of actin-rich stereocilia arranged in a V-shaped staircase pattern on the apical surface of hair cells. The proper formation of this V-shaped structure is critical for facilitating proper hearing [3]. However, the mechanisms that drive proper hair cell function still need to be better understood. The studies of deafness genes improve our understanding of the development and function of hair cells.

Two pathogenic *ELMOD3* gene mutations have been found, leading to either autosomal recessive pre-speech hearing loss or autosomal dominant progressive hearing loss [4, 5]. Our group identified a heterozygous mutation in the *ELMOD3* gene (c.512A>G; p.His171Arg) that segregated with progressive non-syndromic hearing loss in a five-generation Chinese family in an autosomal dominant fashion [5]. *ELMOD3* gene belongs to the engulfment and cell motility family (ELMO family), which consists of six members defined by the presence of the ELMO domain [6]. *ELMOD3* protein is an atypical GTP-activated protein (GAP) for the ARF family and plays roles in multiple cellular functions, including in primary cilia formation and traffic of cargoes from the Golgi to the primary cilium [7, 8]. In rat cochlea, *Elmod3* is highly expressed in the stereocilia, kinocilia and cuticular plate in developing hair cells [4]. Moreover, we found in *Elmod3*<sup>-/-</sup> mice, the absence of *Elmod3* resulted in abnormalities of cochlear hair cells in the manner of shortening and fusion of IHCs' stereocilia and progressive degeneration of OHCs' stereocilia [9]. However, little is known about how disruption of *ELMOD3* mechanistically drives hearing loss.

Thus, using patient-specific human induced pluripotent stem cells (iPSCs) to generate an iPSC-based disease model may provide an approach to studying pathogenesis for hereditary hearing loss [10]. In this study, we generated a patient-specific iPSC line carrying the heterozygous *ELMOD3* c.512A>G mutation for the first time. Besides, we generated an iPSC line from a healthy sibling of the patient as control. The transcriptome analysis was conducted between the patient-specific iPSCs (*ELMOD3*<sup>mut</sup>) and the healthy sibling derived iPSCs (Control). Furthermore, we performed a gene correction of *ELMOD3* c.512A>G mutation iPSCs using CRISPR/Cas9 genome-editing technology, followed by gene profiling and transcriptome sequencing. We found several changes in differential gene expression by comparing the transcriptome of *ELMOD3*<sup>mut</sup> iPSCs and its corrected isogenic control iPSCs (*ELMOD3*<sup>corrected</sup>). It was shown that the *ELMOD3* gene might be involved in biological processes, such as ion homeostasis and sensory epithelial development, etc. We also performed STRING and PPI analysis to predict the potential protein interaction network. Through these data, we could provide supportive evidence for the putative cellular function of the *ELMOD3* gene, thus yielding a model system to study how *ELMOD3* functions in humans to facilitate proper hearing. The overall workflow of this study is shown in Fig 1.

## Materials and methods

### Ethics statement

The Ethics Committee of Xiangya Hospital Central South University (XHCSU) approved the protocol for this study, and signed informed consent was provided by every donor before sample collection. The laboratory research on the derivation and use of human iPSC lines was also approved by XHCSU following local regulations, and all animal experiments were conducted based on XHCSU ethical guidelines.

### Generation and culture of iPSCs

Ten ml of blood was collected from a hearing loss patient with *ELMOD3* c.512A>G mutation and a healthy family member in December 2019 [5]. The generation and culture of iPSCs were performed as described by Wen et al. [11]. The B lymphocytes were isolated from blood and immortalized by EBV. EBV-immortalized B lymphocytes were cultured in RPMI 1640

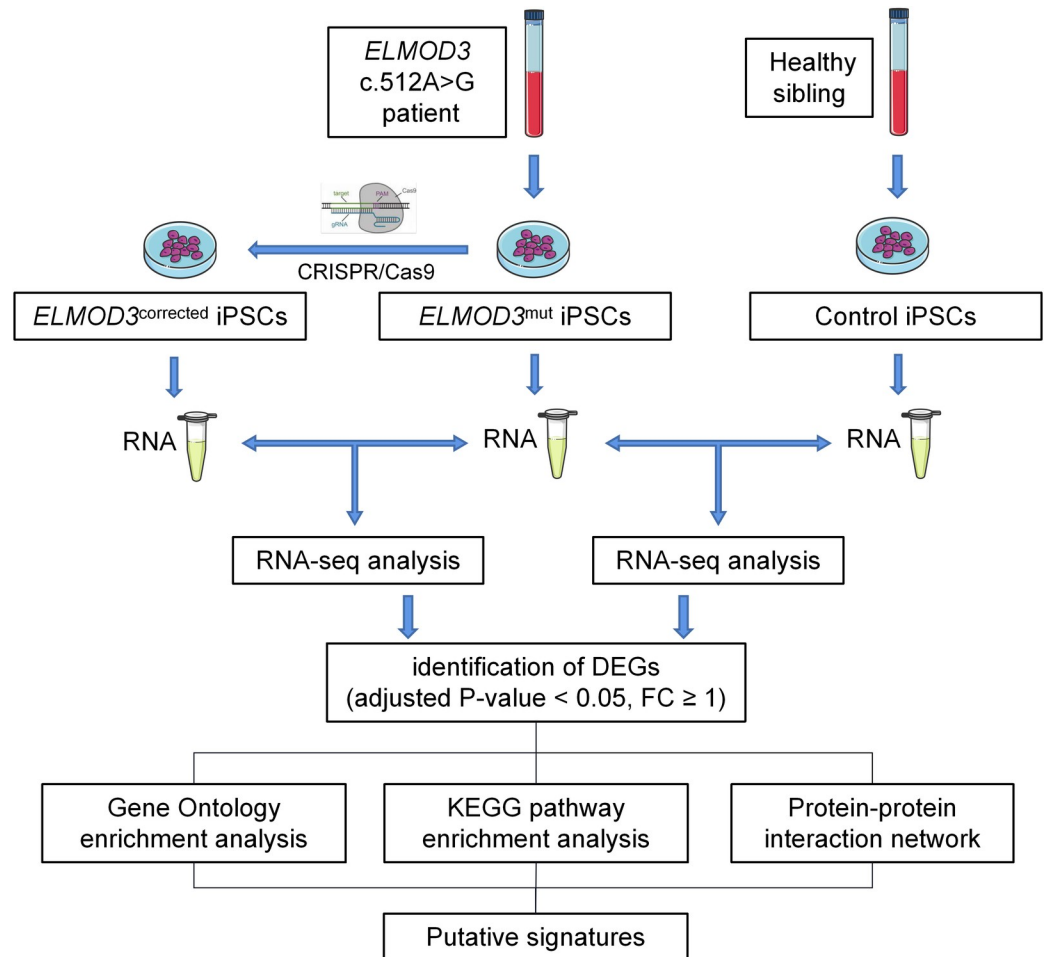


**Fig 1. The overall workflow of this study.**

<https://doi.org/10.1371/journal.pone.0288640.g001>

medium (Gibco, USA) with 10% fetal bovine serum (VISTECH, Australia) and 1 mM sodium pyruvate (Gibco, USA) at 37°C in 5% CO<sub>2</sub>. The expanded EBV-immortalized B lymphocytes were electroporated with two µg per vector of five episomal vectors (Addgene, USA), namely pCXLE-hUL, pCXLEhOCT3/4-shp53-F, pCXLE-hSK, pCXWB-EBNA1, and pCXLE-EGFP, for reprogramming into induced pluripotent stem cells (iPSCs). The Basic Nucleofector™ Kit for Primary Mammalian Epithelial Cells (Lonza, Switzerland) was used for electroporation. After electroporation, the cells were seeded in a 12-well plate and cultured in WiCell + VitC medium (DMEM/F12) (Gibco, USA). The medium should be replaced every 48h. From day 2 to day 12, 0.5 mM sodium butyrate (Sigma, USA) was added to the WiCell + VitC medium. Eight days after transduction, the cells were transferred to mouse embryonic fibroblast-coated 6-well plates at a density of 1.8×10<sup>4</sup> cells per well. From day 12, the medium was changed to WiCell + VitC medium without sodium butyrate. Undifferentiated iPSC colonies were manually picked and transferred onto Matrigel-coated 24-well plates for further expansion.

### sgRNA design

The online tool CHOPCHOP (<http://chopchop.cbu.uib.no/>) was used to design sgRNA. The Lenti CRISPR v2 plasmid designed by Zhang's laboratory was selected as the editing vector.

The DNA fragments were ligated with the digested empty-loading plasmid using a DNA linking kit (Takara, Japan).

### Cell transfections

The four  $\mu\text{g}$  CRISPR/Cas9 targeting plasmids and  $4\mu\text{l}$  ssODN ( $100\mu\text{M}$ ) providing homologous recombination templates were transferred into  $2.5 \times 10^6$  patient-specific iPSCs by electrotransfection. Puromycin resistance genes were used as screening markers to obtain iPSCs successfully transfected. Then, these cells were transferred to culture plates at low density until sufficient clones appeared. Single clones were selected for Sanger sequencing.

### Alkaline phosphatase (AP) staining

Following the manufacturer's instructions, the iPSCs were stained using Alkaline Phosphatase Kit (Beyotime, China). The photography was performed using a Nikon 300 inverted confocal microscope.

### Immunofluorescence staining

Cells were fixed with 4% paraformaldehyde for 20 min, permeabilized using 1% Triton X-100 (Sigma, USA) for 10 min, and blocked with 5% bovine serum albumin (BSA) for 1h. The above processes are carried out at room temperature. Following overnight incubation with primary antibodies in PBS solution with 5% BSA at  $4^\circ\text{C}$ , cells were washed and incubated with appropriate secondary antibodies for 1h at RT in the dark. DAPI (Beyotime, China) was used for nuclear counterstaining, and images were observed and photographed using an Olympus confocal microscope and camera.

### Embryoid body (EB) formation assay

For EB formation, iPSCs were harvested by Accutase (Gibco, USA), and then resuspended in the mTeSR medium (Stemcell Technologies, Canada) supplemented with 20% FBS. The cell suspension was transferred to ultra-low attachment six-well plates and cultured in KO-DMEM (Gibco, USA) supplemented with 20% Knockout Serum Replacement, 1% GlutaMax-I, and 1% nonessential amino acids. The medium should be replaced every 48h. After six days, The suspended spheroid embryoid body was collected and transferred to 6-well plates with gelatin-coated plates. Six days later, total RNA isolated from the embryoid body was reversely transcribed into cDNA for subsequent experiments. The expression of genes in different germ layers was examined by RT-PCR and agarose gel electrophoresis (AGE).

### Teratoma assay

The iPSCs ( $1 \times 10^7$  cells) were harvested by Accutase (Gibco, USA) and injected into the hind limb muscles of 8-week-old male nude mice (Charles River, China). The teratomas were dissected 8 to 10 weeks post-transplantation, fixed with 4% PFA and embedded in paraffin. Tissue sections were stained with hematoxylin and eosin.

### Quantitative reverse transcription-polymerase chain reaction (qRT-PCR)

Total RNA was isolated from cells using the Trizol reagent (Sangon, China). One  $\mu\text{g}$  RNA was reverse transcribed using the PrimeScript™ II 1st Strand cDNA Synthesis Kit (Takara, Japan). The qPCR reactions were performed on Step One plus Real-Time PCR System (ABI) with a 2 $\times$ SYBR Master Mix (Yeasen, China). The relative expression levels of target genes were calculated using the  $2^{-\Delta\Delta\text{Ct}}$  method, and GAPDH served as the internal control.

## RNA sequencing

The total RNA of triple replicates from three samples (*ELMOD3*<sup>mut</sup>, *ELMOD3*<sup>corrected</sup> and healthy control iPSCs) was extracted for further analysis. One µg of total RNA was isolated and used to generate RNA-seq libraries. The library preparations were sequenced on an Illumina Novaseq platform, generating 150 bp paired-end reads. The FPKM of each gene was obtained by quantitative analysis after filtering the raw data and reference genome alignment. Then we selected differentially expressed genes (DEGs) with the DESeq2 method (adjusted P-value < 0.05 and |log<sub>2</sub>(fold-change)| > 1). To discern the implications of DEGs, we performed Gene Ontology (GO) and Kyoto Encyclopedia of Genes and Genomes (KEGG) pathway enrichment and protein-protein interactions (PPI) network analysis on the DEGs. The above analysis used the common online platforms and databases, including Metascape (<http://metascape.org>) [12], KEGG (<http://www.genome.jp/kegg>), the STRING (The Search Tool for the Retrieval of Interacting Genes/Proteins) database (<https://string-db.org/>), and Cytoscape (<http://cytoscape.org/>). The Molecular Complex Detection (MCODE) tool was used to extract functional modules.

## Results

### Generation of a human iPSC line from a patient carrying the heterozygous c.512A>G variant in the *ELMOD3* gene

In our previous study, a heterozygous *ELMOD3* c.512A>G (p.His171Arg) variant was identified as a causative variant in a five-generation Chinese family affected by late-onset and progressive autosomal dominant non-syndromic hearing loss (ADNSHL). The details about hearing loss history and auditory evaluation of the affected members were described previously by Li et al. [5]. Here, we generated two human iPSC lines by reprogramming the donated Epstein-Barr virus (EBV)-immortalized B lymphocytes of two family members (a 59-years-old male patient and his 51-years-old healthy female sibling respectively), henceforth named as *ELMOD3*<sup>mut</sup> and healthy control. Detailed clinical characteristics of these siblings are shown in Table 1.

Both the *ELMOD3*<sup>mut</sup> and the healthy control iPSC lines exhibited a typical pluripotent stem cell-like morphology. The newly raised colonies after the reprogramming process appeared in blue when treated with an AP kit, showing that both iPSC lines presented AP activity and the potential of multi-differentiation (Fig 2A). The two studied clones were positive for NANOG, SOX2 and OCT-4 self-renewal markers, and also positive for SSEA-4 and Tra-1-60 pluripotency surface markers (Fig 2B and 2C). The two iPSCs can differentiate *in vitro* towards the three embryonic germ layers. RT-PCR analyses showed that the embryoid body expressed meaningful marker genes of endoderm, mesoderm and ectoderm (Fig 2E and 2F). Both iPSC lines were competent to differentiate into three germ layers in an *in vivo* teratoma assay (Fig 2G). To summarize, *ELMOD3*<sup>mut</sup> and healthy control iPSC lines exhibited normal iPSC morphology, expressed pluripotency markers and differentiated into cells of three germ layers, which could be used in subsequent experiments.

**Table 1. Clinical characteristics of the patient and the healthy sibling.**

	<i>ELMOD3</i> c.512A > G	Sex	Age	Onset Age	PTA threshold (dBHL)		Tinnitus	Vertigo
					Left	Right		
Patient	Yes	Male	59	37	89	83	No	No
Healthy sibling	No	Female	51	/	30	30	Yes	No

<https://doi.org/10.1371/journal.pone.0288640.t001>

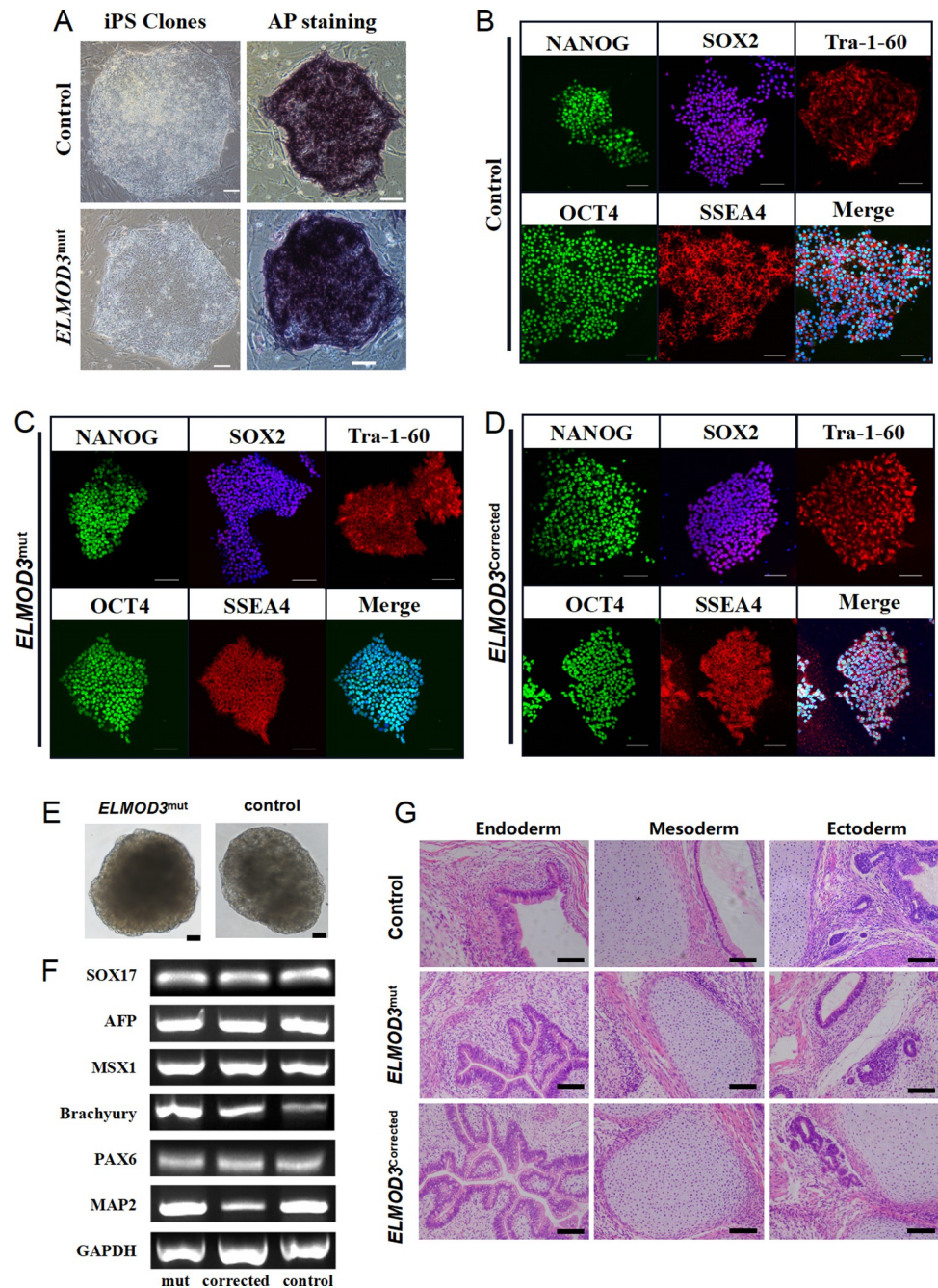


**Fig 2. Generation and characterization of *ELMOD3*<sup>mut</sup>, control and *ELMOD3*<sup>corrected</sup> iPSCs.** (A) The *ELMOD3*<sup>mut</sup> and control iPSC clones show typical embryonic stem cell-like and positive alkaline phosphatase (AP) staining. Bar, 100 $\mu$ M. (B-D) Immunofluorescence staining in all iPSC lines showed expression of pluripotency markers OCT4, NANOG, TRA-1-60, SOX2 and SSEA-4. Bar, 100 $\mu$ M. (E) The *ELMOD3*<sup>mut</sup> and control iPSC line form embryoid body in vitro. Bar, 100 $\mu$ M. (F) The agarose gel electrophoresis of marker genes of three embryonic germ layers in all iPSC lines. (G) HE staining of teratomas generated from subcutaneous injection of all iPSC lines in NOD/SCID mice. Tumor sections represent differentiated structures as noted. Bar, 100 $\mu$ M.

<https://doi.org/10.1371/journal.pone.0288640.g002>

We further observed the nuclear morphology and cytoskeleton of the *ELMOD3*<sup>mut</sup> and healthy control iPSC lines. A high nuclear-cytoplasmic ratio was observed in both iPSC lines, and no significant difference in F-actin density between *ELMOD3*<sup>mut</sup> and healthy control iPSC lines was observed (S1 Fig).

### Global changes in gene expression of the *ELMOD3*<sup>mut</sup> iPSCs carrying the heterozygous c.512A>G mutation

We applied RNA sequencing of the *ELMOD3*<sup>mut</sup> and the healthy control iPSC lines, and a hierarchical cluster heatmap was generated (Fig 3A). The RNA sequencing statistics disclosed that there were 112 differentially expressed transcripts between *ELMOD3*<sup>mut</sup> and control iPSC lines, of which 52 DEGs were up-regulated and 60 DEGs were down-regulated (Fig 3B, S1 and S2 Tables).

We utilized Gene Ontology (GO) analysis to investigate the biological processes associated with the DEGs. The up-regulated genes are mainly enriched in "negative regulation of biological process", "metabolic process", and "response to stimulus" GO terms (Fig 3C). In contrast, among the down-regulated genes caused by the *ELMOD3* c.512A>G mutation, "cellular process", "immune system process", and "metabolic process" are the most significantly enriched GO terms (Fig 3D). Interestingly, both up-regulated and down-regulated genes were enriched in identical biological processes, including the "metabolic process", "response to stimulus", and "developmental process".

However, there were not only *ELMOD3* gene mutations but also genomic differences (such as sex differences) among iPSCs derived from different individuals. Therefore we assume that global changes in gene expression between the above studied iPSC lines could not fully reflect the transcriptomic changes caused by *ELMOD3* c.512A>G mutation in humans.

### CRISPR/Cas9-mediated gene correction in the *ELMOD3*<sup>mut</sup> patient-derived iPSCs

The clustered regularly interspaced short palindromic repeats (CRISPR)/CRISPR-associated protein 9 (Cas9) system is a powerful gene editing tool. Here, we used this system for gene repair in *ELMOD3* patient-derived iPSC line. The Small guide RNAs (sgRNA) were designed using the online tool CHOPCHOP (<http://chopchop.cbu.uib.no/>) and 16 suspicious off-target sequences were selected (see S3 Table for Off-targets sequences, S1A Fig). Sanger sequencing revealed that the *ELMOD3* c.512A>G mutation had been successfully corrected (S3B Fig). Then the 16 sequence regions were validated by PCR amplification and sequencing, showing that none of these 16 suspicious sites occurred (S3C Fig).

The generated iPSC line was named as *ELMOD3*<sup>corrected</sup>. Subsequently, the stemness-related gene expression and pluripotency in the *ELMOD3*<sup>corrected</sup> iPSC were identified. Immunofluorescence staining indicated that the *ELMOD3*<sup>corrected</sup> iPSC line could express the pluripotent stem cell marker NANOG, SOX2, Tra-1-60, OCT4, and SSEA4 (Fig 2D). We also tested its differentiation potential. The *ELMOD3*<sup>corrected</sup> iPSC line can not only form embryos *in vitro*, but also grow in the subcutaneous muscles of NOD-SCID mice, showing that it has multiple differentiation potential (Fig 2G). In conclusion, the *ELMOD3*<sup>corrected</sup> iPSC line has a multi-differentiation potential and was suitable for the following experiments.

### RNA-sequencing analysis of differentially expressed genes (DEGs) between *ELMOD3*<sup>mut</sup> and *ELMOD3*<sup>corrected</sup> iPSC lines

A hierarchical cluster heatmap was generated to analyze the gene expression pattern (Fig 4A). A total of 789 DEGs were identified between *ELMOD3*<sup>mut</sup> and *ELMOD3*<sup>corrected</sup> iPSC lines, of

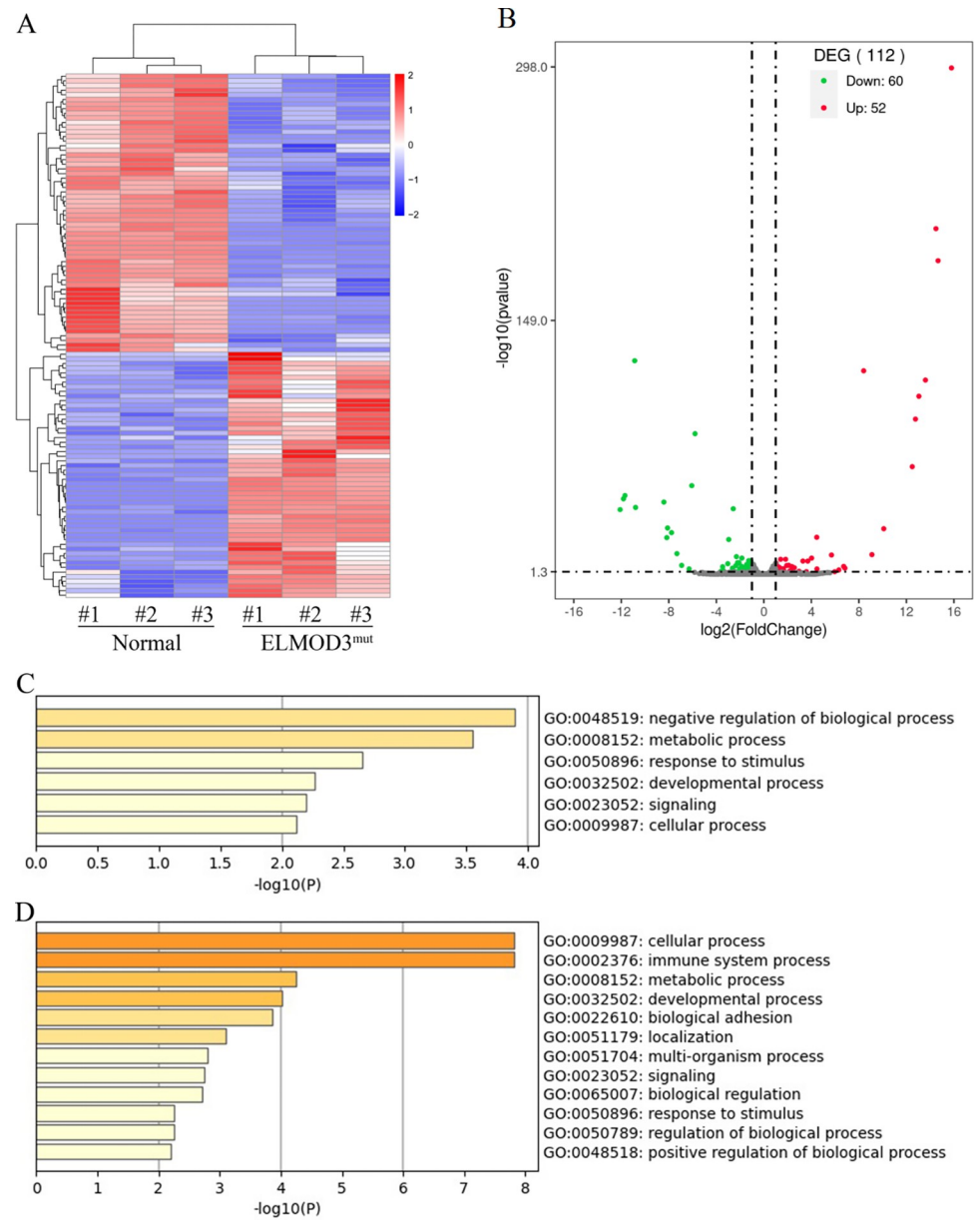


**Fig 3. Differentially expressed genes between *ELMOD3*<sup>mut</sup> and control iPSCs.** (A) The heatmap showed a hierarchical clustering analysis of DEGs in *ELMOD3*<sup>mut</sup> iPSCs. Red and blue indicate genes with high and low expression levels, respectively. (B) Volcano plot showing the expression change of each gene and their significance. Red dots represent the expression of genes in *ELMOD3*<sup>mut</sup> iPSCs significantly up-regulated compared to normal control. Green dots represent the expression of genes in *ELMOD3*<sup>mut</sup> iPSCs significantly down-regulated compared to normal control. (C-D) GO enrichment analysis of differentially expressed genes in *ELMOD3*<sup>mut</sup> iPSCs. GO terms enriched with up-regulated genes are shown in (C). GO terms enriched with down-regulated genes are shown in (D).

<https://doi.org/10.1371/journal.pone.0288640.g003>

which 403 were up-regulated and 386 were down-regulated (Fig 4B, S4 and S5 Tables). We found that *ELMOD3* c.512A>G mutation resulted in significantly down-regulated expression of genes encoding members of the Zinc-finger protein (ZNF) family.

Through GO analysis, 40 GO terms were significantly enriched ( $-\log_{10}$  adjusted P-value > 2). We found that GO terms associated with "biological regulation", "response to stimulus", "developmental process", "growth", and "multicellular organismal process" were most



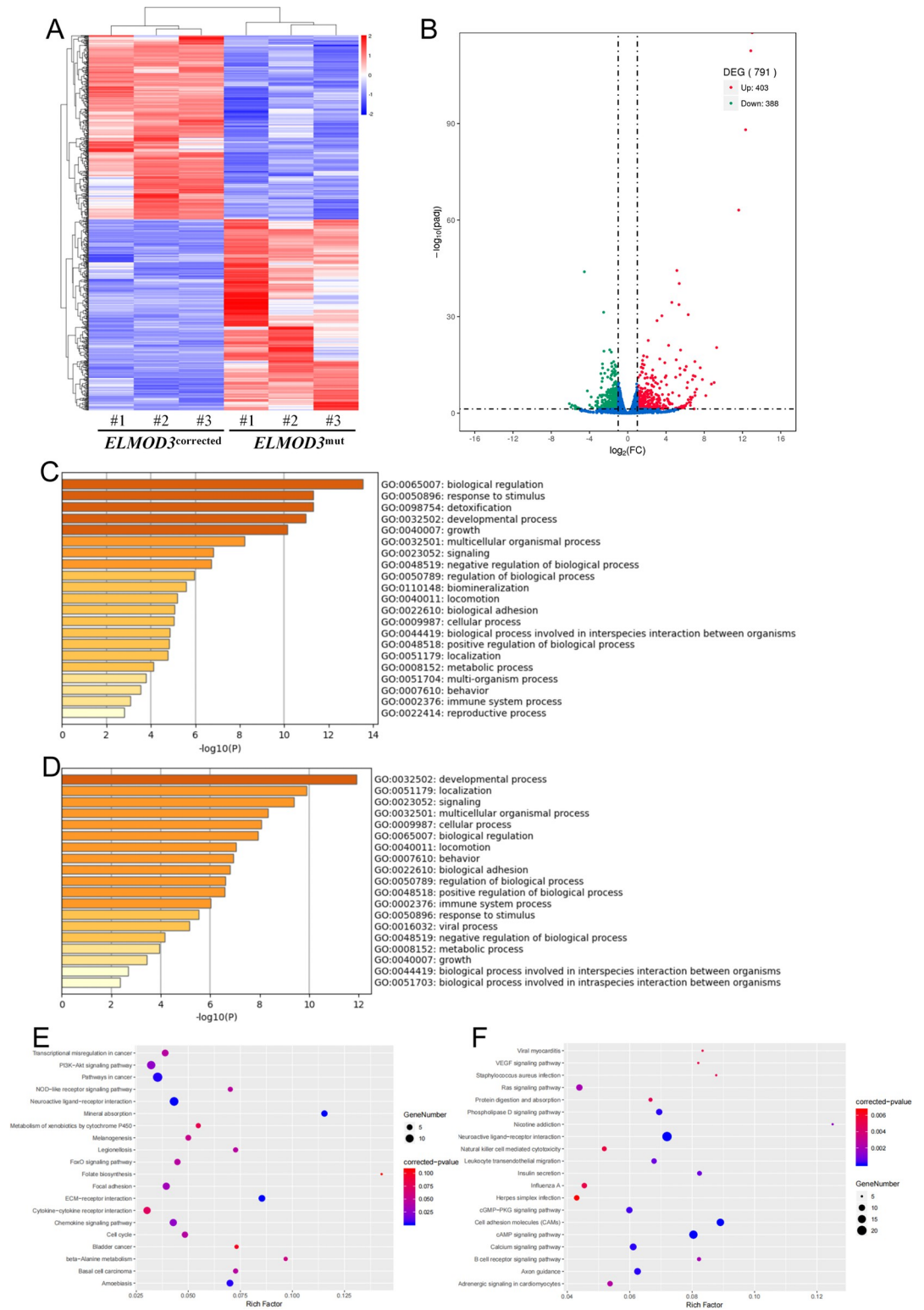


**Fig 4. Differentially expressed genes between *ELMOD3*<sup>mut</sup> and *ELMOD3*<sup>corrected</sup> iPSCs.** (A) The heatmap showed a hierarchical clustering analysis of DEGs between *ELMOD3*<sup>mut</sup> and *ELMOD3*<sup>corrected</sup> iPSCs. Red and blue indicate genes with high and low expression levels, respectively. (B) Volcano plot showing the expression change of each gene and their significance. Red dots represent the expression of genes in *ELMOD3*<sup>mut</sup> iPSCs significantly up-regulated compared to Correction iPSCs. Green dots represent the expression of genes in *ELMOD3*<sup>mut</sup> iPSCs significantly down-regulated compared

to *ELMOD3*<sup>corrected</sup> iPSCs. (C-D) GO enrichment analysis of differently expressed genes between *ELMOD3*<sup>mut</sup> and *ELMOD3*<sup>corrected</sup> iPSCs. GO terms enriched with up-regulated genes are shown in (C). GO terms enriched with down-regulated genes are shown in (D). (E-F) KEGG pathway enrichment analysis of DEGs specific for *ELMOD3*<sup>mut</sup> iPSCs. Pathways enriched with up-regulated genes are shown in (E), while down-regulated genes are in (F).

<https://doi.org/10.1371/journal.pone.0288640.g004>

significantly up-regulated (Fig 4C), while the down-regulated genes were mainly enriched in such as "developmental process", "localization", and "signaling" GO terms (Fig 4D).

Then, we performed KEGG pathway enrichment analysis for down-regulated and up-regulated genes. Focusing on significant enrichments, the up-regulated DEGs were involved mainly in pathways such as "mineral absorption", "neuroactive ligand-receptor interaction", "chemokine signaling pathway", and "PI3K-Akt signaling pathway" (Fig 4E). On the other hand, *ELMOD3*<sup>mut</sup> iPSCs showed enrichment of down-regulated genes for pathways such as "neuroactive ligand-receptor interaction", "cAMP signaling pathway", "calcium signaling pathway", "axon guidance", and "cell adhesion molecules" (Fig 4F).

Furthermore, PPI network analysis of predicted DEGs between *ELMOD3*<sup>mut</sup> and *ELMOD3*<sup>corrected</sup> iPSC lines was performed based on the STRING database. A total of 382 up-regulated genes (Fig 5A) and 361 down-regulated genes (Fig 5G) were mapped to the PPI network. The Molecular Complex Detection (MCODE) tool was used to extract functional modules. Among the up-regulated DEGs, genes related to "GPCR ligand binding", "GPCR downstream signaling", "post-translational protein phosphorylation", "intermediate filament cytoskeleton organization", and "mesenchyme migration" were significantly enriched (Fig 5B–5F). The down-regulated DEGs were most significantly enriched in "GPCR ligand binding", "cAMP signaling pathway", "ephrin receptor signaling pathway", "chloride transport", and "neuroactive ligand-receptor interaction" (Fig 5H–5L).

It is worth noting that, among the up-regulated DEGs in this study, one module included a total of 7 genes: *MYL7*, *TNNI3*, *VIM*, *PRPH*, *NEFL*, *KCNMA1*, and *ACTG2* was associated with "intermediate filament cytoskeleton organization" (Fig 5E), whereas another module consisted of a total of 6 genes: *ACTC1*, *ACTA1*, *ACTA2*, *ALDHA3*, *BTF3*, and *SLC25A6* were mainly enriched in "mesenchyme migration" (Fig 5F). Amongst these DEGs, four genes were tested in a qRT-PCR assay and the expression of tested genes was significantly up-regulated in *ELMOD3*<sup>mut</sup> iPSCs, which was consistent with the RNA-seq results (S3A and S3B Fig). These findings echo our earlier research that defects in the *Elmod3* gene caused the inner ear hair cell stereocilia structural abnormalities *in mice*.

Moreover, we also found DEGs related to neural development and ion transport, especially potassium ion transport. There were 26 down-regulated genes linked to "regulation of ion transmembrane transport", including *LRRC55*, *CACNG8*, *NOS1AP*, *KCNH2*, *GJA5*, etc., of which 16 genes linked to "potassium ion transport" including *KCNB1*, *KCNC3*, *KCNG1*, *KCNH2*, *KCNK2*, *KCNN3*, and *KCNN4* (Fig 6, left). In the *ELMOD3*<sup>mut</sup> iPSC line, genes related to "sensory organ development", especially "ear morphogenesis" were significantly up-regulated, including *TBX1*, *ATOH1* and *ALDH1A3* etc. (Fig 6, right). We verified the expression levels of several of these genes by qRT-PCR, and the result was also consistent with RNA-seq results (S3C–S3F Fig).

## Discussion

Hearing loss (HL) is one of the world's most common sensory deficits with exceptionally high genetic heterogeneity [13]. 50% to 60% of hearing loss in babies is due to genetic causes [14]. Different mutations at one causative gene could result in different patterns of inheritance and various phenotypes. For example, *ELMOD3* mutation (c.794 T>C; p.Leu265Ser) is responsible

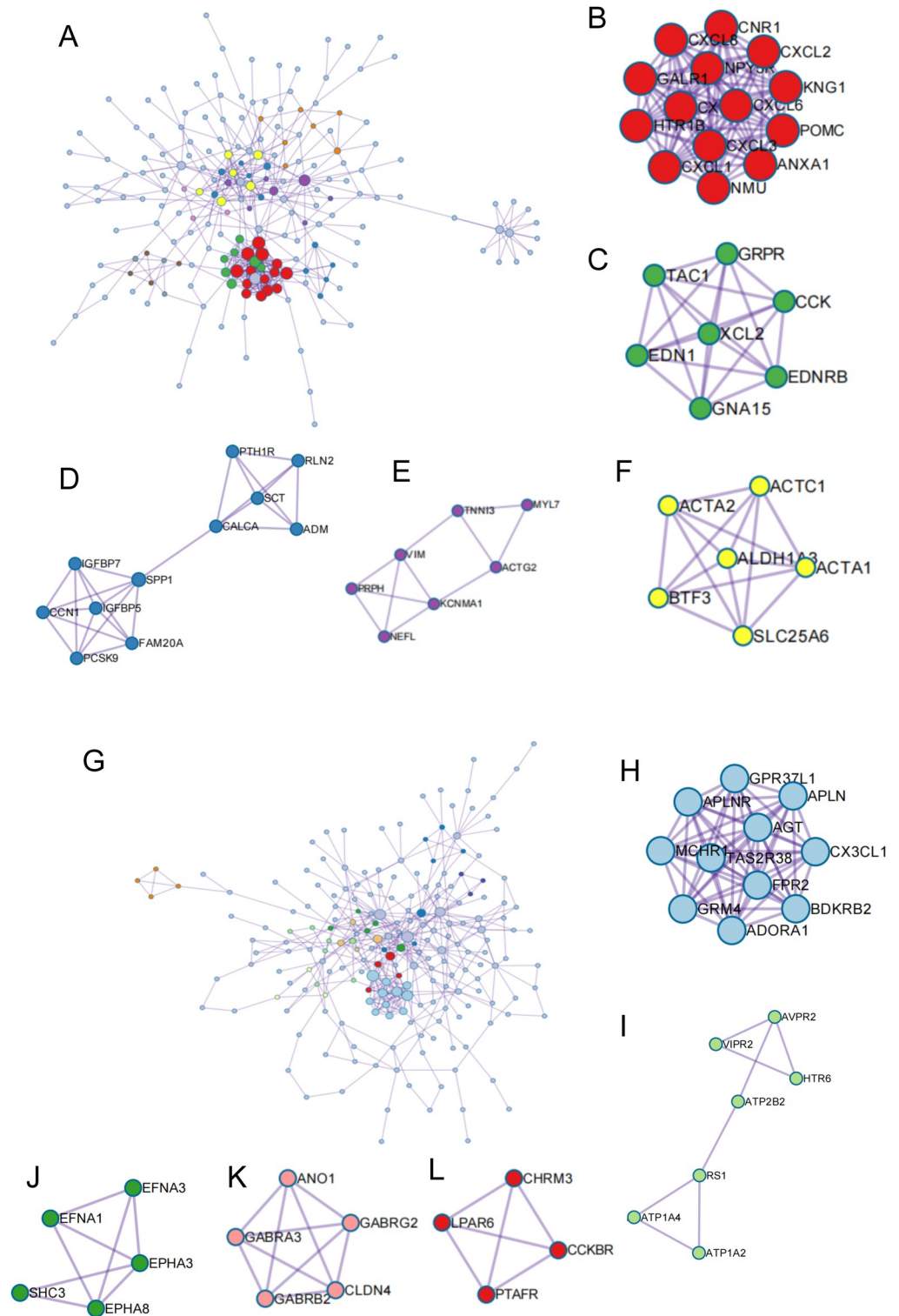


**Fig 5. PPI network analysis of total DEGs in *ELMOD3*<sup>mut</sup> and *ELMOD3*<sup>corrected</sup> iPSCs.** (A-F) PPI network of up-regulated DEGs and modules 1–5 identified from the whole PPI network. (A) the whole PPI network of up-regulated DEGs. (B) GPCR ligand binding. (C) GPCR downstream signalling. (D) Post-translational protein phosphorylation. (E) Ntermediate filament cytoskeleton organization. (F) mesenchyme migration. (G-L) PPI network of down-regulated DEGs and modules 1–5 identified from the whole PPI network. (G) the whole PPI network of down-regulated DEGs. (H) GPCR ligand binding. (I) cAMP signaling pathway. (J) Ephrin receptor signaling pathway. (K) Chloride transport. (L) Neuroactive ligand-receptor interaction.

<https://doi.org/10.1371/journal.pone.0288640.g005>

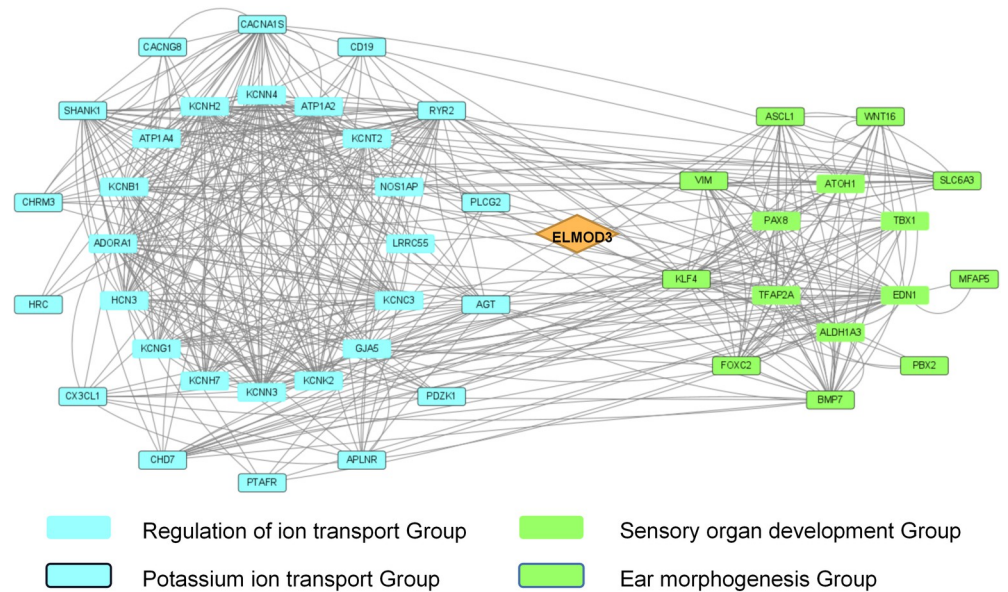


**Fig 6. Integrated analysis of specific gene sets in DEGs of *ELMOD3*<sup>mut</sup> and *ELMOD3*<sup>corrected</sup> iPSCs.** The diamond represents *ELMOD3*. The blue square represents the genes enriched in the GO term regulation of ion transport, and the blue square with the frame indicates genes related to potassium ion transport. The green square represents the genes enriched in the GO term sensory organ development, and the green square with the frame indicates genes related to ear morphogenesis.

<https://doi.org/10.1371/journal.pone.0288640.g006>

for autosomal recessive non-syndromic HL and another *ELMOD3* mutation (c.512A>G; p. His171Arg) causes non-syndromic progressive HL in an autosomal dominant fashion [4, 5]. Deafness genes, such as *GJB2* and *TMC1*, show similar clinical manifestations [15–18]. In this case, it is necessary to carry out a series of animal and cell studies on different mutation sites for these genes.

The *ELMOD3* protein belongs to the engulfment and cell motility family (ELMO family), which has the same ELMO domain. The human ELMO protein family consists of six members, which could be further divided into two subgroups, ELMOs and ELMODs, based on protein size and domain architecture [6]. The ELMOD proteins share GAP activity and a conserved ELMO domain, a ~160 residue domain also present in human ELMO proteins [7, 19]. The c.512A>G mutation in the *ELMOD3* gene was found in amino acid 171, substituting a highly conserved histidine residue with arginine [5]. In a previous study, we confirmed that *Elmod3*<sup>-/-</sup> mice exhibited progressive hearing loss and hair cells stereocilia morphology anomalies [9]. Whereas the mechanisms underlying stereocilia morphology anomalies are still not fully understood. There are many differences in phenotype between animal and human models due to differences in genetic background, organ development timelines, and underlying regulatory mechanisms between species [20, 21]. Therefore, in this study we chose to generate patient-specific human iPSCs carrying c.512A>G mutation, which could be used as an iPSC-based disease model for pursuing how disruption of *ELMOD3* causes hearing loss.

Since 1998, when Thomson and his colleagues reported the first human embryonic stem cell lines [22], iPSCs have led to a better understanding of the mechanisms that mediate normal and abnormal early human development. Personalized iPSC lines can be derived, enabling studies of the molecular pathogenesis of inherited diseases [23]. Given the inner ear's complex cellular and molecular structure, and all cell types within the inner ear are present in small amounts, iPSC-based modeling of hearing and hearing loss promises to revolutionize scientific

approaches to hearing loss [24]. In the past few years, iPSCs have begun to play an important role in illuminating the details of human inner ear development, particularly the formation of functional hair cells [25, 26].

In the current work, we successfully reprogrammed B lymphocytes from a hearing loss patient with *ELMOD3* c.512A>G mutation into iPSCs, based on the Yamanaka method [27]. The iPSCs cell model established in this study is not only an effective tool to study how disruption of *ELMOD3* mechanistically drives hearing loss, but also provides a potential tool to carry out gene therapy research in the future. To our knowledge, this is the first documented disease model of induced pluripotent stem cells from deafness patients caused by an *ELMOD3* gene mutation.

When new iPSC lines are developed, it is essential to perform exhaustive characterization of the new lines [28]. We have carried out a panel of assays, including morphological observation, AP activity detection, pluripotency marker expression, and teratoma formation potential. The results showed that *ELMOD3* mutant iPSCs exhibited similar pluripotency properties as control iPSCs. A comprehensive transcriptome profiling of iPSCs from patients with the heterozygous *ELMOD3* c.512A>G mutation was performed using next-generation RNA-Sequencing. Compared to control iPSCs, transcriptome analysis of *ELMOD3*<sup>mut</sup> iPSCs showed that there were 112 DEGs significantly altered. However, the DEGs in the above transcriptomics analysis could be biased due to different gender and other genomic differences between this patient and his healthy sister. For example, the top 5 up-regulated genes of *ELMOD3*<sup>mut</sup> iPSCs were located on the Y chromosome (*RPS4Y1*, *KDM5D*, *USP9Y*, *NLGN4Y* and *EIF1AY*).

In order to exclude such differences in gene expression profiles between different individuals, we also generate a corrected isogenic control iPSCs (*ELMOD3*<sup>corrected</sup>) using CRISPR/Cas9 technology, which is based on the single-guide RNA (sgRNA) encoding DNA-binding specificity and combined with a single nuclease (Cas9) [29]. Sanger sequencing revealed that the *ELMOD3* c.512A>G mutation was successfully corrected, and no off-targeting had occurred. After genetic correction with CRISPR/Cas9, the *ELMOD3*<sup>corrected</sup> iPSCs retained the multiple differentiation potential. Compared with the control iPSCs, several genes located on the Y chromosome whose expression was significantly up-regulated in the *ELMOD3*<sup>corrected</sup> iPSCs (S6 Table). Of the 35 up-regulated genes shared between *ELMOD3*<sup>mut</sup> group (*ELMOD3*<sup>mut</sup> vs control) and *ELMOD3*<sup>corrected</sup> group (*ELMOD3*<sup>corrected</sup> vs control), 11 were located on the Y chromosome. This indicates that gender factors should be considered in transcriptome analysis if different gender samples are used.

Transcriptome comparison between *ELMOD3*<sup>mut</sup> and *ELMOD3*<sup>corrected</sup> iPSC lines revealed more exciting findings. The transcriptional landscapes of the above two studies are quite different, while we still find some features in common, such as two sets of DEGs were both enriched in "response to stimulus" and "developmental process". It should be noted that compared to *ELMOD3*<sup>corrected</sup> iPSCs, the *ELMOD3* c.512A>G mutations led to the up-regulation of genes associated with the biological process "sensory epithelial development". Moreover, previous studies showed that *ELMOD3* was expressed in the stereocilia of hair cells in rat and mouse models [4, 9], and defects in the *ELMOD3* gene lead to morphological abnormalities of the hair cells' stereocilia in mice [9]. Deletion of *Elmod1* *in vitro* results in the decreased ability of cells to form primary cilia, and the loss of a subset of proteins from cilia [8]. *ELMOD3* interacts with Rab1A and Flotillin2 to regulate lumen formation via vesicle trafficking [30]. The current work found a series of DEGs related to sensory epithelial development and cytoskeleton organization through functional enrichment and PPI network analysis, including *ATOH1*, *VIM*, *PRPH* and *NEFL*, which may be involved in the pathogenesis of *ELMOD3* causing deafness.

*ATOH1* (*Atonal BHLH Transcription Factor 1*) plays a crucial role in hair cell development and maturation [31]. *Atoh1*<sup>-/-</sup> mice exhibited severe hearing loss and vestibular dysfunction,

with complete loss of cochlear hair cells and vestibular hair cells [32]. In E15.5-E17.5, *Atoh1* depletion resulted in rapid hair cell death, but the removal of *Atoh1* after this period did not affect the number of new hair cells [33]. Overexpression of *Atoh1* induces hair cell regeneration in the adult cochlea [34]. Our study showed that *ELMOD3* mutation resulted in increased expression of *ATOH1*. This may be the compensation for the effects of *ELMOD3* mutations. However, with the cochlea's maturation, cochlear cells' ability to respond to *Atoh1* will be gradually weakened [35]. Whether *ELMOD3* and *ATOH1* interacted with each other is worth exploring in future studies. Furthermore, previous studies on the mechanism of *ELMOD3* induced deafness mainly focused on abnormal stereocilia morphology. *Loi et al.* found that *ELMOD3-SH2D6* gene fusion leads to autism spectrum disorders [36], which suggests that the *ELMOD3* gene has more functions yet to be discovered.

We also found that several DEGs linked to the biological process "potassium ion transport" were significantly down-regulated. Hereditary progressive hearing loss is closely related to decreased cell surface expression and impaired potassium channel conductance in outer hair cells [37]. The human genome contains roughly 70  $K^+$  channel-encoding genes [38]. Many of these genes play essential roles in auditory processes, such as *KCNQ4* [39], *KCNQ1* [40], *KCNMA1* [41] and so on. They are expressed in different parts of the cochlea and play different roles. In both studied transcriptome analyses, *LRR55* expression was significantly down-regulated. *LRR55* belongs to large conductance  $K^+$  channels, termed BK channels, which play an essential role in cell excitability and maintenance of  $K^+$  homeostasis [42]. BK channel expression has been identified in the cell bodies of SGN and hair cells [41, 43]. Compared to *ELMOD3*<sup>corrected</sup> iPSCs, there were 26 down-regulated genes linked to "regulation of ion transmembrane transport" and 16 genes linked to "potassium ion transport" were down-regulated in the *ELMOD3*<sup>mut</sup> iPSC line. These results suggest that *ELMOD3* might be involved in regulating cochlear  $K^+$  homeostasis.

In summary, we generated a patient-specific iPSC line carrying *ELMOD3* c.512A>G mutation and a healthy control iPSC line for the first time. Subsequently, the patient-specific iPSCs were corrected by CRISPR/Cas9. In addition, we applied transcriptome profiling to compare these iPSC lines. In-depth analysis of high throughput RNA sequencing data between the patient-specific iPSCs and the corrected iPSCs, we attempt to know more about how disruption of *ELMOD3* mechanistically drives hearing loss. Although we should acknowledge that this study is based only on transcript levels, our current work provided a new tool for studying the cellular function of *ELMOD3* and gave hints about biological processes which may be related to *ELMOD3*. *ELMOD3* may affect the process of sensory epithelial development and the regulation of ion transmembrane transport via some other proteins. Thus, more extensive studies and awareness of these associations are needed. Also, if inner-ear-like tissue could be derived from these iPSC lines in the next step, coupled with transcriptome and proteome profiling could be conducted at that stage, we could further extend our understanding of the molecular etiology of *ELMOD3* causing hearing loss.

## Supporting information

**S1 Fig. Immunofluorescence staining of the nuclear morphology and cytoskeleton of all iPSC lines.** Bar, 100 $\mu$ M.

(TIF)

**S2 Fig. Establishment of correction of the *ELMOD3* gene in patient-derived iPSCs with CRISPR/Cas9.** (A) The schematic of gDNA targeting and mutation site G is highlighted in red. (B) Sanger sequencing confirmed that the *ELMOD3* mutation had been corrected successfully. The original heterozygous mutation was replaced by a new nonsense mutation. C(+/+):

control iPSC. P(+/-): *ELMOD3*<sup>mut</sup> iPSCs. P(+/+): *ELMOD3*<sup>corrected</sup> iPSCs. (C) Sequencing results of 16 possible off-target sites.  
(TIF)

**S3 Fig. qRT-PCR validation of the transcript levels of three group genes.** Black bars indicate relative gene expression in *ELMOD3*<sup>corrected</sup> iPSCs and gray bars in *ELMOD3*<sup>mut</sup> iPSCs. All data are presented as the means±SD; the P-value was calculated by t-test. \*: P < 0.05; \*\*: P < 0.01; \*\*\*: P < 0.001. (A-B) Intermediate filament cytoskeleton organization and mesenchyme migration group. (C-D) Ear morphogenesis group. (E-F) Potassium ion transport group.  
(TIF)

**S4 Fig. Differentially expressed genes between *ELMOD3*<sup>corrected</sup> and control iPSCs.** (A) The heatmap showed a hierarchical clustering analysis of DEGs between *ELMOD3*<sup>corrected</sup> and control iPSCs. Red and blue indicate genes with high and low expression levels, respectively. (B) Volcano plot showing the expression change of each gene and their significance. Red dots represent the expression of genes in *ELMOD3*<sup>corrected</sup> iPSCs significantly up-regulated compared to normal control. Green dots represent the expression of genes in *ELMOD3*<sup>corrected</sup> iPSCs significantly down-regulated compared to normal control. (C-D) Venn diagram representing the quantity of shared genes between group A (*ELMOD3*<sup>mut</sup> vs control) and group B (*ELMOD3*<sup>corrected</sup> vs control).  
(TIF)

**S1 Table. The list of up-regulated genes between *ELMOD3*<sup>mut</sup> and control iPSC lines.**  
(XLSX)

**S2 Table. The list of down-regulated genes between *ELMOD3*<sup>mut</sup> and control iPSC lines.**  
(XLSX)

**S3 Table. 16 off-target sequences.**  
(PDF)

**S4 Table. The list of up-regulated genes between *ELMOD3*<sup>mut</sup> and *ELMOD3*<sup>corrected</sup> iPSC lines.**  
(XLSX)

**S5 Table. The list of down-regulated genes between *ELMOD3*<sup>mut</sup> and *ELMOD3*<sup>corrected</sup> iPSC lines.**  
(XLSX)

**S6 Table. The list of up-regulated genes between *ELMOD3*<sup>corrected</sup> and control iPSC lines.**  
(XLSX)

**S7 Table. The list of down-regulated genes between *ELMOD3*<sup>corrected</sup> and control iPSC lines.**  
(XLSX)

**S1 Raw images. The original images.**  
(TIF)

## Author Contributions

**Conceptualization:** Jie Wen, Xuezhong Liu, Chufeng He, Lingyun Mei, Jie Ling, Yong Feng.

**Data curation:** Xianlin Liu, Jie Wen, Xuezhong Liu, Sijun Li, Wei Gong, Chufeng He.

**Formal analysis:** Xianlin Liu, Jing Liu, Xiaoming Kang, Zhili Feng, Lingyun Mei, Jie Ling, Yong Feng.

**Funding acquisition:** Lingyun Mei, Yong Feng.

**Investigation:** Xianlin Liu, Jie Wen, Sijun Li, Jing Liu, Jie Sun, Chufeng He.

**Methodology:** Xuezhong Liu, Jie Sun, Zhili Feng, Lingyun Mei, Jie Ling, Yong Feng.

**Project administration:** Yong Feng.

**Resources:** Xuezhong Liu, Jie Sun, Chufeng He, Lingyun Mei, Yong Feng.

**Software:** Anhai Chen, Jing Liu, Jie Sun, Zhili Feng, Jie Ling.

**Supervision:** Jie Wen, Anhai Chen, Sijun Li, Wei Gong, Xiaoming Kang.

**Validation:** Jie Wen, Anhai Chen, Sijun Li, Jing Liu, Wei Gong, Xiaoming Kang.

**Visualization:** Anhai Chen, Jing Liu.

**Writing – original draft:** Xianlin Liu, Anhai Chen, Zhili Feng, Jie Ling.

**Writing – review & editing:** Xianlin Liu, Jie Wen, Xuezhong Liu, Anhai Chen, Zhili Feng, Jie Ling, Yong Feng.

## References

1. Shim K. The auditory sensory epithelium: the instrument of sound perception. *Int J Biochem Cell Biol.* 2006; 38(11): 1827–33. <https://doi.org/10.1016/j.biocel.2006.03.012> PMID: 16814589
2. Cheatham MA. Cochlear function reflected in mammalian hair cell responses. *Prog Brain Res.* 1993; 97: 13–19. [https://doi.org/10.1016/s0079-6123\(08\)62258-x](https://doi.org/10.1016/s0079-6123(08)62258-x) PMID: 8234739
3. Wagner EL, Shin JB. Mechanisms of Hair Cell Damage and Repair. *Trends Neurosci.* 2019; 42(6): 414–424. <https://doi.org/10.1016/j.tins.2019.03.006> PMID: 30992136
4. Jaworek TJ, Richard EM, Ivanova AA, Giese AP, Choo DI, Khan SN, T, et al. An alteration in *ELMOD3*, an Arl2 GTPase-activating protein, is associated with hearing impairment in humans. *PLoS Genet.* 2013; 9(9): e1003774. <https://doi.org/10.1371/journal.pgen.1003774> PMID: 24039609
5. Li W, Sun J, Ling J, Li J, He C, Liu Y, et al. *ELMOD3*, a novel causative gene, associated with human autosomal dominant nonsyndromic and progressive hearing loss. *Hum Genet.* 2018; 137(4): 329–342. <https://doi.org/10.1007/s00439-018-1885-0> PMID: 29713870
6. East MP, Bowzard JB, Dacks JB, Kahn RA. ELMO domains, evolutionary and functional characterization of a novel GTPase-activating protein (GAP) domain for Arf protein family GTPases. *J Biol Chem.* 2012; 287(47): 39538–39553. <https://doi.org/10.1074/jbc.M112.417477> PMID: 23014990
7. Ivanova AA, East MP, Yi SL, Kahn RA. Characterization of recombinant *ELMOD* (cell engulfment and motility domain) proteins as GTPase-activating proteins (GAPs) for ARF family GTPases. *J Biol Chem.* 2014; 289(16): 11111–11121. <https://doi.org/10.1074/jbc.M114.548529> PMID: 24616099
8. Turn RE, Hu Y, Dewees SI, Devi N, East MP, Hardin KR, et al. The ARF GAPs *ELMOD1* and *ELMOD3* act at the Golgi and cilia to regulate ciliogenesis and ciliary protein traffic. *Mol Biol Cell.* 2022; 33(2): ar13. <https://doi.org/10.1091/mbc.E21-09-0443> PMID: 34818063
9. Li W, Feng Y, Chen A, Li T, Huang S, Liu J, et al. *Elmod3* knockout leads to progressive hearing loss and abnormalities in cochlear hair cell stereocilia. *Hum Mol Genet.* 2019; 28(24): 4103–4112. <https://doi.org/10.1093/hmg/ddz240> PMID: 31628468
10. Hosoya M, Fujioka M, Sone T, Okamoto S, Akamatsu W, Ukai H, et al. Cochlear Cell Modeling Using Disease-Specific iPSCs Unveils a Degenerative Phenotype and Suggests Treatments for Congenital Progressive Hearing Loss. *Cell Rep.* 2017; 18(1): 68–81. <https://doi.org/10.1016/j.celrep.2016.12.020> PMID: 28052261
11. Wen J, Song J, He C, Ling J, Liu Y, Chen H, et al. Establishment of an iPSC line (CSUXHi003-A) from a patient with Waardenburg syndrome type II caused by a *MITF* mutation. *Stem Cell Res.* 2021; 51: 102157. <https://doi.org/10.1016/j.scr.2021.102157> PMID: 33454628



12. Zhou Y, Zhou B, Pache L, Chang M, Khodabakhshi AH, Tanaseichuk O, et al. Metascape provides a biologist-oriented resource for the analysis of systems-level datasets. *Nat Commun.* 2019; 10(1): 1523. <https://doi.org/10.1038/s41467-019-09234-6> PMID: 30944313
13. Acharya A, Schrauwen I, Leal SM. Identification of autosomal recessive nonsyndromic hearing impairment genes through the study of consanguineous and non-consanguineous families: past, present, and future. *Hum Genet.* 2022; 141(3–4): 413–430. <https://doi.org/10.1007/s00439-021-02309-9> PMID: 34291353
14. Kenna MA. Acquired Hearing Loss in Children. *Otolaryngol Clin North Am.* 2015; 48(6): 933–953. <https://doi.org/10.1016/j.otc.2015.07.011> PMID: 26452421
15. Morell RJ, Kim HJ, Hood LJ, Goforth L, Friderici K, Fisher R, et al. Mutations in the connexin 26 gene (*GJB2*) among Ashkenazi Jews with nonsyndromic recessive deafness. *N Engl J Med.* 1998; 339(21): 1500–1505. <https://doi.org/10.1056/NEJM199811193392103> PMID: 9819448
16. Wang HY, Zhao YL, Liu Q, Yuan H, Gao Y, Lan L, et al. Identification of Two Disease-causing Genes *TJP2* and *GJB2* in a Chinese Family with Unconditional Autosomal Dominant Nonsyndromic Hereditary Hearing Impairment. *Chin Med J (Engl).* 2015; 128(24): 3345–3351. <https://doi.org/10.4103/0366-6999.171440> PMID: 26668150
17. Gao X, Huang SS, Yuan YY, Wang GJ, Xu JC, Ji YB, et al. Targeted gene capture and massively parallel sequencing identify *TMC1* as the causative gene in a six-generation Chinese family with autosomal dominant hearing loss. *Am J Med Genet A.* 2015; 167A(10): 2357–2365. <https://doi.org/10.1002/ajmg.a.37206> PMID: 26079994
18. Imtiaz A, Maqsood A, Rehman AU, Morell RJ, Holt JR, Friedman TB, et al. Recessive mutations of *TMC1* associated with moderate to severe hearing loss. *Neurogenetics.* 2016; 17(2): 115–123. <https://doi.org/10.1007/s10048-016-0477-1> PMID: 26879195
19. Bowzard JB, Cheng D, Peng J, Kahn RA. *ELMOD2* is an *Arl2* GTPase-activating protein that also acts on *Arfs*. *J Biol Chem.* 2007; 282(24): 17568–17580. <https://doi.org/10.1074/jbc.M701347200> PMID: 17452337
20. Doncheva NT, Palasca O, Yarani R, Litman T, Anthon C, Groenen MAM, et al. Human pathways in animal models: possibilities and limitations. *Nucleic Acids Res.* 2021; 49(4): 1859–1871. <https://doi.org/10.1093/nar/gkab012> PMID: 33524155
21. Chen Y, Zhang S, Chai R, Li H. Hair Cell Regeneration. *Adv Exp Med Biol.* 2019; 1130: 1–16. [https://doi.org/10.1007/978-981-13-6123-4\\_1](https://doi.org/10.1007/978-981-13-6123-4_1) PMID: 30915698
22. Thomson JA, Itskovitz-Eldor J, Shapiro SS, Waknritz MA, Swiergiel JJ, Marshall VS, et al. Embryonic stem cell lines derived from human blastocysts. *Science.* 1998; 282(5391): 1145–7. <https://doi.org/10.1126/science.282.5391.1145> PMID: 9804556
23. Hockemeyer D, Jaenisch R. Induced Pluripotent Stem Cells Meet Genome Editing. *Cell Stem Cell.* 2016; 18(5): 573–86. <https://doi.org/10.1016/j.stem.2016.04.013> PMID: 27152442
24. Stojkovic M, Han D, Jeong M, Stojkovic P, Stankovic KM. Human induced pluripotent stem cells and CRISPR/Cas-mediated targeted genome editing: Platforms to tackle sensorineural hearing loss. *Stem Cells.* 2021; 39(6): 673–696. <https://doi.org/10.1002/stem.3353> PMID: 33586253
25. Whitfield TT. Development of the inner ear. *Curr Opin Genet Dev.* 2015; 32: 112–8. <https://doi.org/10.1016/j.gde.2015.02.006> PMID: 25796080
26. Koehler KR, Nie J, Longworth-Mills E, Liu XP, Lee J, Holt JR, et al. Generation of inner ear organoids containing functional hair cells from human pluripotent stem cells. *Nat Biotechnol.* 2017; 35(6): 583–589. <https://doi.org/10.1038/nbt.3840> PMID: 28459451
27. Takahashi K, Yamanaka S. Induction of pluripotent stem cells from mouse embryonic and adult fibroblast cultures by defined factors. *Cell.* 2006; 126(4): 663–76. <https://doi.org/10.1016/j.cell.2006.07.024> PMID: 16904174
28. Aasen T, Raya A, Barrero MJ, Garreta E, Consiglio A, Gonzalez F, et al. Efficient and rapid generation of induced pluripotent stem cells from human keratinocytes. *Nat Biotechnol.* 2008; 26(11): 1276–84. <https://doi.org/10.1038/nbt.1503> PMID: 18931654
29. Jinek M, Chylinski K, Fonfara I, Hauer M, Doudna JA, Charpentier E. A programmable dual-RNA-guided DNA endonuclease in adaptive bacterial immunity. *Science.* 2012; 337(6096): 816–21. <https://doi.org/10.1126/science.1225829> PMID: 22745249
30. Liu A, Ouyang X, Wang Z, Dong B. *ELMOD3*-Rab1A-Flotillin2 cascade regulates lumen formation via vesicle trafficking in *Ciona* notochord. *Open Biol.* 2023; 13(3): 220367. <https://doi.org/10.1098/rsob.220367> PMID: 36918025
31. Zhong C, Fu Y, Pan W, Yu J, Wang J. *Atoh1* and other related key regulators in the development of auditory sensory epithelium in the mammalian inner ear: function and interplay. *Dev Biol.* 2019; 446(2): 133–141. <https://doi.org/10.1016/j.ydbio.2018.12.025> PMID: 30605626

32. Bermingham NA, Hassan BA, Price SD, Vollrath MA, Ben-Arie N, Eatock RA, et al. Math1: an essential gene for the generation of inner ear hair cells. *Science*. 1999; 284(5421): 1837–41. <https://doi.org/10.1126/science.284.5421.1837> PMID: 10364557
33. Cai T, Seymour ML, Zhang H, Pereira FA, Groves AK. Conditional deletion of *Atoh1* reveals distinct critical periods for survival and function of hair cells in the organ of Corti. *J Neurosci*. 2013; 33(24): 10110–22. <https://doi.org/10.1523/JNEUROSCI.5606-12.2013> PMID: 23761906
34. Atkinson PJ, Wise AK, Flynn BO, Nayagam BA, Richardson RT. Hair cell regeneration after *ATOH1* gene therapy in the cochlea of profoundly deaf adult guinea pigs. *PLoS One*. 2014; 9(7): e102077. <https://doi.org/10.1371/journal.pone.0102077> PMID: 25036727
35. Kelly MC, Chang Q, Pan A, Lin X, Chen P. *Atoh1* directs the formation of sensory mosaics and induces cell proliferation in the postnatal mammalian cochlea in vivo. *J Neurosci*. 2012; 32(19): 6699–710. <https://doi.org/10.1523/JNEUROSCI.5420-11.2012> PMID: 22573692
36. Loi E, Moi L, Blois S, Bacchelli E, Vega Benedetti AF, Cameli C, et al. *ELMOD3-SH2D6* gene fusion as a possible co-star actor in autism spectrum disorder scenario. *J Cell Mol Med*. 2020; 24(2): 2064–2069. <https://doi.org/10.1111/jcmm.14733> PMID: 31800155
37. Peixoto Pinheiro B, Vona B, Löwenheim H, Rüttiger L, Knipper M, Adel Y. Age-related hearing loss pertaining to potassium ion channels in the cochlea and auditory pathway. *Pflugers Arch*. 2021; 473(5): 823–840. <https://doi.org/10.1007/s00424-020-02496-w> PMID: 33336302
38. González C, Baez-Nieto D, Valencia I, Oyarzún I, Rojas P, Naranjo D, et al. K(+) channels: functional overview. *Compr Physiol*. 2012; 2(3): 2087–149. <https://doi.org/10.1002/cphy.c110047> PMID: 23723034
39. Kubisch C, Schroeder BC, Friedrich T, Lütjohann B, El-Amraoui A, Marlin S, et al. *KCNQ4*, a novel potassium channel expressed in sensory outer hair cells, is mutated in dominant deafness. *Cell*. 1999; 96(3): 437–46. [https://doi.org/10.1016/s0092-8674\(00\)80556-5](https://doi.org/10.1016/s0092-8674(00)80556-5) PMID: 10025409
40. Barhanin J, Lesage F, Guillemare E, Fink M, Lazdunski M, Romey G. K(V)LQT1 and *IsK* (minK) proteins associate to form the I(Ks) cardiac potassium current. *Nature*. 1996; 384(6604): 78–80. <https://doi.org/10.1038/384078a0> PMID: 8900282
41. Hafidi A, Beurg M, Dulon D. Localization and developmental expression of BK channels in mammalian cochlear hair cells. *Neuroscience*. 2005; 130(2): 475–84. <https://doi.org/10.1016/j.neuroscience.2004.09.038> PMID: 15664704
42. Schumacher MA, Rivard AF, Bächinger HP, Adelman JP. Structure of the gating domain of a Ca<sup>2+</sup>-activated K<sup>+</sup> channel complexed with Ca<sup>2+</sup>/calmodulin. *Nature*. 2001; 410(6832): 1120–4. <https://doi.org/10.1038/35074145> PMID: 11323678
43. Skinner LJ, Enée V, Beurg M, Jung HH, Ryan AF, Hafidi A, et al. Contribution of BK Ca<sup>2+</sup>-activated K<sup>+</sup> channels to auditory neurotransmission in the Guinea pig cochlea. *J Neurophysiol*. 2003; 90(1): 320–32. <https://doi.org/10.1152/jn.01155.2002> PMID: 12611976